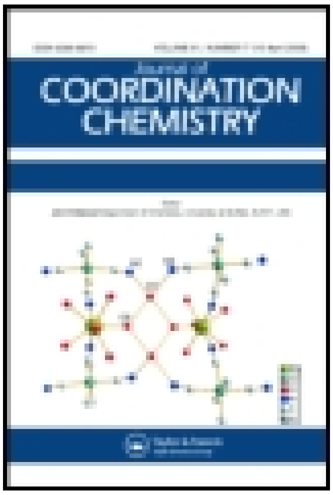

Journal of Coordination Chemistry
Publication details, including instructions for authors and subscription information:
http://www.tandfonline.com/loi/gcoo20

Nickel(II), copper(II), cobalt(II) and palladium(II) complexes with a Schiff base: Crystal structure, DFT study and copper complex catalyzed aerobic oxidation of alcohol to aldehyde

Kuladip Sarma[a], Namita Devi[a], Mukul Kalita[a], Bipul Sarma[b] & Pranjit Barman[a]
[a] Department of Chemistry, National Institute of Technology, Silchar 788010, Assam, India
[b] Department of Chemical Sciences, Tezpur University, Tezpur 784028, Assam, India
Accepted author version posted online: 29 Jul 2015.

To cite this article: Kuladip Sarma, Namita Devi, Mukul Kalita, Bipul Sarma & Pranjit Barman (2015): Nickel(II), copper(II), cobalt(II) and palladium(II) complexes with a Schiff base: Crystal structure, DFT study and copper complex catalyzed aerobic oxidation of alcohol to aldehyde, Journal of Coordination Chemistry, DOI: 10.1080/00958972.2015.1075241

To link to this article: http://dx.doi.org/10.1080/00958972.2015.1075241

Publisher: Taylor & Francis

Journal: *Journal of Coordination Chemistry*

DOI: http://dx.doi.org/10.1080/00958972.2015.1075241

Nickel(II), copper(II), cobalt(II) and palladium(II) complexes with a Schiff base: Crystal structure, DFT study and copper complex catalyzed aerobic oxidation of alcohol to aldehyde

KULADIP SARMA†, NAMITA DEVI†, MUKUL KALITA†, BIPUL SARMA‡ and PRANJIT BARMAN*†

†Department of Chemistry, National Institute of Technology, Silchar 788010, Assam, India
‡Department of Chemical Sciences, Tezpur University, Tezpur 784028, Assam, India

Ni(II), Cu(II), Co(II) and Pd(II) complexes were synthesized with a Schiff base containing thioether with ONS-donors chelating to the metal center. The ligand and complexes were characterized by elemental analysis, FT-IR, ^{1}H-NMR, UV-visible spectroscopy and magnetic studies. The crystal structures of the ligand and its Ni(II) and Pd(II) complexes were determined by single-crystal X-ray diffraction analysis. The structure reveals that ligand-chelated Ni(II) and Pd(II) in slightly distorted octahedral and slightly distorted square planar environment, respectively. DFT studies of the Pd(II) complex reveal that the calculated structural parameters are very close with the experimentally observed data. The Cu(II) complex shows very good catalytic activity towards conversion of alcohol to aldehyde under aerobic oxidation with ammonium persulfate.

Keywords: Schiff base; Crystal structure; Catalytic activities; DFT Study

1. Introduction

Schiff bases have influenced coordination chemistry [1] because they have good coordinating ability to form stable complexes with most transition metal ions. Such behavior of Schiff base offered opportunities for inducing substrate chirality, tuning metal centered electronic factors, enhancing stability of either homogeneous or heterogeneous catalyst [2-11]. Schiff base metal

*Corresponding author. barmanpranjit@yahoo.co.in

complexes with nitrogen-sulfur donors are important because they mimic biologically significant metalloenzymes [12]. Also, Schiff bases form charge-transfer complexes with O and N with the aid of metals like Ni, Cu and Co showing the importance as enzyme models. The rapid development of these types of ligands have enhanced research activity in coordination chemistry. Metal complexes with ONS-donors show antitumor, fungicidal, bactericidal, antibacterial, antifungal, anti-inflammatory and antiviral activities [13-22]. Ni(II) Schiff base complexes efficiently catalyze C-S cross-coupling of thiols with organic chlorides [23]. Ni(II) complexes of chelating ligands incorporating thioether and imine donors have relevant properties with various metalloproteins such as blue copper proteins, hemocyanin, tyrosinase and metalloenzymes as well as their stability [24-26]. Pd(II) complexes with ONS donor Schiff bases also have wide catalytic activity in organic transformations such as polymerization of ethylene, epoxidation, allylic alkylation, Heck reaction, Suzuki–Miyaura coupling reactions, *etc*. [27-31]. Moreover, Cu(II) Schiff base complexes are used as versatile catalysts in various oxygenation reactions in homogeneous as well as heterogeneous conditions [32].

The oxidation of alcohol to aldehyde is an important reaction in organic chemistry. Numerous reagents and methods are reported for these conversions [33-47], but development of environmentally benign processes are a challenge. Cu(II) complexes are useful metal mediated catalysts in these conversions.

Here we synthesize a Schiff base from 2-hydroxynaphthaldehyde and 2-(benzylthio)aniline and a series of metal complexes with Cu(II), Ni(II), Co(II) and Pd(II) ions. We have also studied catalytic activity of the Cu(II) complex towards aerobic oxidation of alcohol to aldehyde in acetonitrile by using ammonium persulfate as oxidant.

2. Experimental

2.1. *Materials*

All chemicals were used without purification. Nickel chloride hexahydrate, copper nitrate trihydrate and cobalt acetate tetrahydrate were purchased from Merck India and 2-hydroxynaphthaldehyde and sodium tetrachloropalladate were purchased from Alfa Aesar. All alcohols were purchased from Aldrich. 2-(Benzylthio)aniline was prepared according to literature method [48]. Solvents used were extra pure grade purchased from Merck India and were dried by the reported procedure [49].

2.2. *Methods*

Infrared spectra of the ligand and complexes were recorded with a FT-IR-3000 Hyperion Microscope (Bruker, Germany). Elemental analyses were performed on a Flash 2000 Thermo Scientific instrument. ^{1}H-NMR spectra of the ligand and Pd(II) complex were performed on a VARIAN Mercury plus 300 MHz NMR spectrometer using $CDCl_3$ as solvent. Electrical conductivities were measured on a CM-180 Conductivity meter (Elico India). Electronic spectra of the compounds were carried out with a Cary 100 Bio UV-visible spectrometer in DMF. Magnetic susceptibilities were measured on a conventional Gouy balance using freshly prepared $Hg[Co(NCS)_4]$ as calibrant using a Magway MSB MK1 Magnetic susceptibility balance, Sherwood Scientific, Cambridge, UK. Melting points were recorded on a Veego melting point apparatus and were uncorrected.

2.3. *Synthesis of ligand HL (1)*

2-(Benzylthio)aniline (0.215 g, 1 mmol) was dissolved in ethanol. To the above solution, an ethanolic solution of 2-hydroxynaphthaldehyde (0.172 g, 1 mmol) was added dropwise with continuous stirring. The resulting solution was allowed to stir for 30 min at room temperature. The color of the solution changed to dark yellow. The solution was kept at 0 °C for 4 h; a yellow crystalline product formed, was filtered off, washed with 25% ethanol-water and dried in vacuum (10^{-2} torr). The product was recrystallized in ethanol, giving suitable crystals for single crystal X-ray diffraction analysis. Yield was almost quantitative. M.P: 185 °C. IR (KBr, cm^{-1}) 3435 (m), 1610 (s), 1457 (s), 1167 (s), 743 (s). ^{1}H-NMR ($CDCl_3$, 300 MHz): δ 15.30 (1H, s, OH), 9.2 (1H, s, CH=N), 7.1-8.09 (12H, m, Ar-H), 4.1 (2H, s, CH_2). UV-Vis [DMF, λ_{max}, nm (ε_{max}, $M^{-1}cm^{-1}$)]: 267 (15600), 319 (9490), 392 (11250), 466 (4020). Anal. Calc. for $C_{24}H_{19}NOS$: C, 78.02; H, 5.18; N, 3.79; S, 8.68; O, 4.33. Found: C, 77.95; H, 5.31; N, 3.82; S, 8.54; O, 4.90.

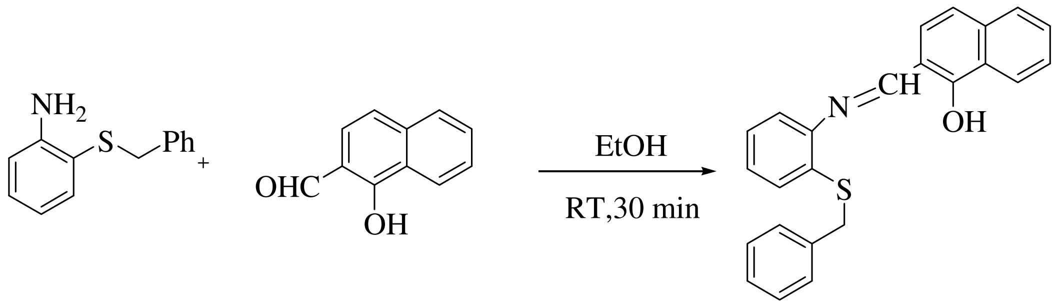

Scheme 1. Synthesis of **HL** (**1**).

2.4. ***Synthesis of complexes***

2.4.1. Synthesis of [NiL_2] (2). HL (**1**) (0.738 g, 2 mmol) was dissolved in hot methanol followed by addition of a methanolic solution of NaOH (0.08 g, 2 mmol). A hot methanolic solution of $NiCl_2·6H_2O$ (0.237 g, 1 mmol) was added drop-by-drop to the above solution with continuous stirring. The reaction mixture was stirred for 1 h and color of the solution changed to dark brown. Concentrating to half volume and storing for 3-4 days at room temperature gave a dark brown needle-type crystal suitable for single-crystal X-ray diffraction analysis. The crystals were washed several times with 25% methanol-water to remove impurities and dried under vacuum at 10^{-2} torr (Purity was checked by TLC). Yield 65%; MP: > 300 °C. IR (KBr, cm^{-1}): 1604 (s), 1455 (s), 1167 (s), 750 (s). UV-Vis [DMF, λ_{max}, nm (ε_{max}, $M^{-1}cm^{-1}$)]: 281 (20450), 331 (18050), 496 (15000), 601 (160). Conductivity (λ_M, S cm^2mol^{-1}): 18.3. Anal. Calc. for $C_{48}H_{36}N_2O_2S_2Ni$: C, 72.46; H, 4.56; N, 3.52; S, 8.06; O, 4.02. Found: C, 71.89; H, 4.10; N, 3.88; S, 7.87; O, 3.95.

2.4.2. Synthesis of [$Cu_2L_2(NO_3)_2$] (3). Complex **3** was prepared by the same procedure as **2** with **HL** (**1**) (0.369 g, 1 mmol), NaOH (0.04 g, 1 mmol) and $Cu(NO_3)_2·3H_2O$ (0.199 g, 1 mmol). The color of the solution changed to dark-green and was kept for 2 days. A green precipitate was collected, washed with 25% methanol-water and dried under vacuum at 10^{-2} torr (Purity was checked by TLC). Yield 62%; MP: > 300 °C. IR (KBr, cm^{-1}): 1604 (s), 1440 (s), 1297 (s), 1150 (s), 741 (s). UV-Vis [DMF, λ_{max}, nm (ε_{max}, $M^{-1}cm^{-1}$)]: 275 (19650), 320 (17250), 413 (11300), 652 (120). Conductivity (λ_M, Scm^2mol^{-1}): 21.7. Anal. Calc. for $C_{48}H_{36}N_4O_8S_2Cu_2$: C, 58.35; H, 3.67; N, 5.67; S, 6.49; O, 12.95. Found: C, 57.79; H, 4.11; N, 5.43; S, 6.21; O, 12.58.

2.4.3. Synthesis of [CoL_2] (4). Complex **4** was prepared by the same procedure as **2** with $Co(CH_3COO)_2 \cdot 4H_2O$ (0.249 g, 1 mmol). The color of the solution changed to red and was kept for 2 days. A black precipitate was collected, washed with 25% methanol-water and dried at 10^{-2} torr (Purity was checked by TLC). Yield 70%; MP: >300 °C. IR (KBr, cm^{-1}): 1603 (s), 1455 (s), 1170 (s), 749 (s). UV-Vis [DMF, λ_{max}, nm (ε_{max}, $M^{-1}cm^{-1}$)]: 281 (13400), 322 (5625), 485 (2410), 624 (500). Conductivity (λ_M, Scm^2mol^{-1}): 26. Anal. Calc. for $C_{48}H_{36}N_2O_2S_2Co$: C, 72.44; H, 4.56; N, 3.52; S, 8.06; O, 4.02. Found: C, 72.80; H, 4.98; N, 2.77; S, 7.12; O, 4.55.

2.4.4. Synthesis of [PdLCl]·0.5(CH_2Cl_2) (5). An ethanolic solution of Na_2PdCl_4 (0.147 g, 0.5 mmol) was added dropwise to an ethanolic solution of **HL** (**1**) (0.185 g, 0.5 mmol). The resulting solution was stirred under reflux for 1 h. The orange precipitate formed was filtered off and washed with 25% ethanol-water solution several times to remove impurities and dried under vacuum (10^{-2} torr) (Purity was checked by TLC). Orange red, needle-like crystals suitable for single crystal X-ray diffraction analysis were obtained by recrystallization from DCM-hexane (10:1) followed by slow evaporation of the solvent (2 days). Yield 68%; MP: > 300 °C. IR (KBr, cm^{-1}): 1604 (s), 1459 (s), 1170 (s), 746 (s). ^{1}H-NMR ($CDCl_3$, 300 MHz): δ 8.95 (1H, s, CH=N), 7.10-7.75 (13 H, m, Ar-H), 4.53 and 4.34 (2H, dd, CH_2). UV-Vis [DMF, λ_{max}, nm (ε_{max}, $M^{-1}cm^{-1}$)]: 268 (7965), 347 (3000), 356 (3100), 444 (2575), 472 (2500). Conductivity (λ_M, Scm^2mol^{-1}): 24.1. Anal. Calc. for [$C_{24}H_{18}NOSPdCl$]·0.5(CH_2Cl_2): C, 53.23; H, 3.46; N, 2.53; S, 5.80; O, 2.89. Found: C, 53.39; H, 3.40; N, 2.45; S, 5.64; O, 2.74.

2.5. ***General procedure for Cu(II) complex catalyzed aerobic oxidation of alcohol to aldehyde***

Here we have reported aerobic oxidation of alcohol to aldehyde using **3**. In this method, substrate (4 mmol), 5 mol % Cu(II) complex and ammonium persulfate (5 mmol) were added to 20 mL acetonitrile. The reaction mixture was stirred at room temperature. The conversion takes place within 2 min and the progress of the reaction was monitored by TLC. The product was extracted with EtOAc and purified by column chromatography. The reaction scheme is shown in scheme 2.

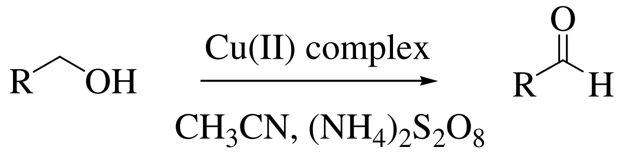

Scheme 2. Oxidation of alcohol to aldehyde.

2.6. ***Crystallography***

All data were collected on a Bruker APEX-II CCD diffractometer with graphite monochromated Cu Kα radiation by the ω-scan technique at 298 K (**HL** (**1**)), 100 K (**2**) and 296 K (**5**). Structures were determined using SHELXS-97 [50, 51]. Cell measurement and data reduction were done by Bruker SAINT [52]. Multi-scan method (SADABS) was used for absorption corrections [52]. Full matrix least-squares on F^2 were performed using the SHELXS-97 program. All non-H atoms were refined in anisotropic approximation using reflections with $I>2\sigma$ (I). Crystal data and structure refinements of **1**, **2** and **5** are given in table 1.

2.7. ***DFT calculation***

Full geometry optimization of Pd(II) complex was performed using Gaussian 09W [53]. Structural calculation was carried out using B3LYP method and mixed basis sets of LanL2DZ for Pd and 6-31+G(d) for all other atoms, *i.e.* Cl, S, N, O, C and H.

3. Results and discussion

3.1. ***Synthesis***

The reactions of ONS-donor Schiff base ligand with corresponding metal salts are shown in scheme 3. **HL** (**1**) binds with nickel and cobalt ions with a 2:1 molar ratio forming octahedral geometry around the metal. However, physicochemical analyses reveal the Cu(II) complex has five-coordinate binuclear square pyramidal geometry around Cu(II). A new FT-IR band around 1297 cm^{-1} was observed for coordinated nitrate in **3**. The Pd(II) complex shows distorted square planar geometry. Molar conductivity studies reveal that the metal complexes are non-electrolytes. The reaction scheme is shown in scheme 3.

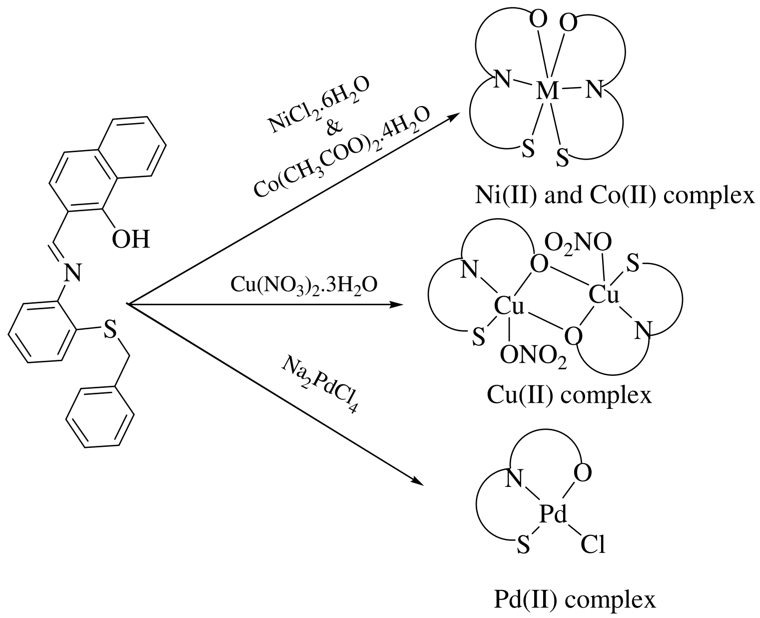

Scheme 3. Synthesis of metal complexes.

3.2. ***[1]H-NMR spectra of HL (1) and [PdLCl]·0.5(CH$_2$Cl$_2$) (5)***

The ^{1}H-NMR (300 MHz) spectra of **HL** and **5** were recorded in $CDCl_3$. A singlet for phenolic OH is at 15.317 ppm for **HL**, shifted downfield due to the presence of phenol-amine hydrogen bonding. A singlet for benzilidemine proton is at 9.22 ppm. The aromatic (Ar-H) and benzylic (CH_2) protons are a multiplet and singlet at 7.1-8.09 ppm and 4.1 ppm, respectively.

In the spectrum of Pd(II) complex, the OH proton disappears, signifying the deprotonation upon complexation. Peaks at 8.95 ppm, 7.12-7.88 ppm and 4.45 ppm appeared for CH=N, aromatic protons and CH_2 protons, respectively. The methylene proton appeared as two separate doublets having germinal-coupling.

3.3. ***Magnetic measurements***

The magnetic moment (μ_{eff}) for Ni(II) complex is 2.80 BM, near to the expected value of d^8 octahedral symmetry. The binuclear Cu(II) complex possesses magnetic moment value of 1.62 BM, smaller than spin-only value [54]; the Co(II) complex shows magnetic moment of 4.81 BM for high-spin octahedral symmetry and the Pd(II) complex is diamagnetic.

3.4. *Electronic spectra*

Electronic spectra of the ligand at 10^{-4} M and complexes at 2×10^{-4} M in DMF are shown in figure 1. Electronic spectra of the ligand and its complexes are also taken in higher concentrations (10^{-3} M) for the region 500-800 nm, shown as insets in figure 1. The electronic spectrum of ligand shows peaks at 267, 319, 392 and 466 nm which may be assigned to π-π* transitions for the phenyl ring and n-π* transitions of the imine moiety [55]. Electronic transitions of complexes are grouped in different spectral zones: 268-281 nm due to π-π* transition of the phenyl ring, 320-356 nm of complexes due to n-π* transition and 413-496 nm may be assigned to MLCT. Complexes show a relatively weak absorption from 601-652 nm due to ligand field transitions, except the Pd(II) complex. All electronic spectral data of **1**-**5** are given in table 2.

3.5. *X-ray crystallography*

The crystal of **HL** (**1**) was obtained by recrystallization from extra pure ethanol and **5** was obtained through slow diffusion of hexane into DCM solution. Prospective view of molecular structure of **1**, **2** and **5** are given in figures 2-4.

Compound **1** crystallizes in the tetragonal space group P4(1). The C=N bond length provides evidence of formation of azomethine group (1.295(6) Å as N(1)-C(7)) in the range of normal C=N bond lengths of imines. The angles N(1)-C(7-C(8) and C(6)-N(1)-C(7) are 122.2(4)° and 122.7(4)° and suggest that the 2-hydroxynaphthyl moiety and N-methyl benzamine are *trans* to each other and reside in the same plane. The benzylsulfanyl unit forms *trans*-geometry about the imine double bond to form ONS donor chelate. All important bond lengths and angles of **1** are given in table 3.

Compound **2** crystallizes in the triclinic space group P-1 containing one molecule in the asymmetric unit. The crystal shows lower R, wR and bond length e.s.d values compare to the reported one [55], indicating better crystallographic data [56]. Two deprotonated ligand units coordinate through $N_2S_2O_2$-donors forming octahedral Ni(II) complex. The C—N, C—S and C—O bond lengths in Ni(II) complex are shifted compared to the free ligand. The imine bond N(3)—C(27) increases to 1.308(3) Å from 1.295(6) Å and S(2)—C(21) increases to 1.839(2) Å from 1.821(5) Å due to donation of electron cloud of N and S to nickel. However, the O(1)—C(11) bond decreases to 1.287(3) Å from 1.343(6) Å due to the delocalization of negative charge of deprotonated oxygen to the ligand, acquiring partial double bond character. The two deprotonated oxygens of two ligands bonded to Ni(II) are *cis* to each other and two sulfurs also *cis*. These four donors are the basal plane and two nitrogens are axial at an angle N(3)—Ni(1)—N(2), 173.43(7)°. The bite angles O(1)—Ni(1)—O(4), O(4)—Ni(1)—S(2), O(1)—Ni(1)—S(3) and S(2)—Ni(1)—S(3) are 93.03(6)°, 92.54(4)°, 84.66(4)° and 90.910(19)°, respectively. All the bite angles deviate from 90°, indicating that the Ni(II) complex has distorted octahedral geometry. All the important bond lengths and angles of **2** are given in table 4.

Complex **5** crystallizes in the monoclinic space group P2(1)/c containing two molecules in the asymmetric unit. One DCM molecule is also observed in the asymmetric unit of the crystal lattice. Important bond lengths and angles of **5** are given in table 5. The Pd—S and Pd—O bond lengths show regular Pd—S and Pd—O bond lengths [57]. Pd(II) coordinates with O, N and S of the ligand and one Cl^- to fulfill the square planar geometry. The bite angles O(1)—Pd(1)—Cl(1), S(1)—Pd(1)—Cl(1), O(2)—Pd(2)—N(2) and N(2)—Pd(2)—S(2) are 89.1(2)°, 90.60(10)°, 93.0(4)° and 87.0(3)°, respectively; angles N(1)—Pd(1)—Cl(1) and O(2)—Pd(2)—S(2) at 175.8(3)° and 179.5(3)° confirm slightly distorted square planar geometry.

3.6. *Cu(II) complex catalyzed aerobic oxidation of alcohol to aldehyde*

The reaction conditions were optimized by performing a series of experiments with different solvents, oxidants, catalysts and reaction time. The optimized reaction conditions for benzyl alcohol and results are shown in table 6; 5 mol% Cu(II) complex as catalyst and 5 mmol ammonium persulfate as oxidant were optimum concentrations for conversion of 4 mmol benzyl alcohol to benzyldehyde in 20 mL acetonitrile. The oxidation reaction was performed for different alcohols as shown in table 7. **3** exhibits very good catalytic activity with high yield at room temperature.

We proposed the mechanism of binuclear Cu(II) complex catalyzed oxidation of primary alcohol to aldehyde. Cu(II)Cu(II) binuclear complex undergoes reduction to intermediate Cu(I)Cu(I) form without breaking the oxobridge [58] in CH_3CN and oxidizes alcohol to aldehyde. Here, $(NH_4)_2S_2O_8$ enhances the formation of molecular oxygen in the system and helps the conversion of Cu(I)Cu(I) to Cu(II)Cu(II) by releasing water as byproduct to complete the catalytic cycle [59-63]. The reaction takes place by two electron transfer from alcohol to binuclear Cu(II)Cu(II) complex. Intermediate Cu(I)Cu(I) is stabilized by CH_3CN, hence the reaction is efficient. The probable mechanism for oxidation of alcohol is given in scheme 4.

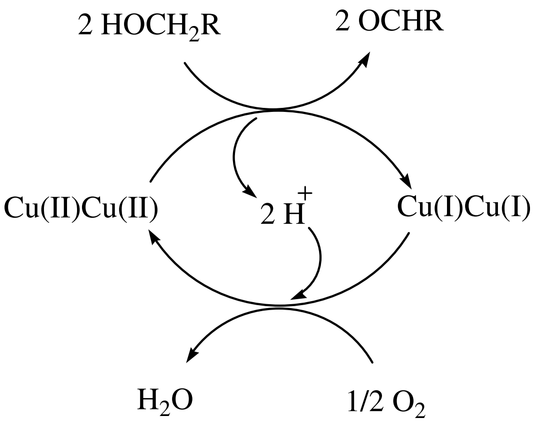

Scheme 4. Probable mechanism for oxidation of alcohol to aldehyde.

3.7. ***DFT calculation***

The optimized geometry of **5** was performed by DFT/B3LYP method. The calculated bond distances and angles are included in table 8. The calculated structural parameters are in agreement with the experimentally observed data. The Pd-S bond of the complex shows maximum deviation of 0.072 Å compared with other metal-atom bonds. The contour plots of HOMO-1, HOMO, LUMO and LUMO + 1 of the complex are shown in figure 5.

4. Conclusion

We have synthesized a tridentate ONS-donor and four complexes and characterized by spectral and single-crystal X-ray diffraction analysis. Complexes **2** and **4** have the 2:1 ratio of tridentate ligand:metal ion and **3** and **5** have the 1:1 ratio of tridentate ligand:metal ion. The geometry of the Ni(II) complex is slightly distorted octahedral and Pd(II) complex is slightly distorted square planar. We have developed a catalytic system using the Cu(II) complex and $(NH_4)_2S_2O_8$ for selective oxidation of alcohol to aldehyde in acetonitrile. The system is attractive due to simple procedure, environmentally benign, high yield within shorter reaction at room temperature. The DFT study of the Pd(II) complex **5** using B3LYP method show quite good agreement with the data obtained from single-crystal X-ray diffraction studies.

Appendix A. Supplementary data

CCDC 997116, 997117 and 997118 contains the supplementary crystallographic data for the ligand, the Ni(II) complex and the Pd(II) complex, respectively. These data can be obtained free of charge via http://www.ccdc.cam.ac.uk/conts/retrieving.html or from the Cambridge Crystallographic Data Centre, 12 Union Road, Cambridge CB2 1EZ, UK; Fax: (+44) 1223-336-033; or E-mail: deposit@ccdc.cam.ac.uk.

Acknowledgements

The authors gratefully acknowledge Indian Association for the Cultivation of Science, Kolkata for the Gaussian 09 program package, Tezpur University, Tezpur and IIT Bombay, Mumbai for spectral and analytical data. Also thanks to Director of NIT, Silchar for financial assistance (K.S, N.D and M.K).

References

[1] Z.L. You, H.L. Zhu. *Z. Anorg. Allg. Chem.*, **630**, 2754 (2004).

[2] K.P. Balasubramanian, K. Parameswari, V. Chinnusamy, R. Prabhakaran, K. Natarajan. *Spectrochim. Acta, Part A*, **65**, 678 (2006).

[3] K.S. Murray, A.M. van den Bergen, B.O. West. *Aust. J. Chem.*, **31**, 203 (1978).

[4] H. Doine, F.F. Stephens, R.D. Cannon. *Bull. Chem. Soc. Jpn.*, **58**, 1327 (1985).

[5] K. Nakajima, Y. Ando, H. Mano, M. Kojima. *Inorg. Chim. Acta*, **274**, 184 (1998).

[6] B.D. Clercq, F. Verpoort. *Macromolecules*, **35**, 8943 (2002).

[7] T. Opstal, F. Verpoort. *Synlett*, **6**, 0935 (2002).

[8] T. Opstal, F. Verpoort. *Angew. Chem. Int. Ed.*, **42**, 2876 (2003).

[9] S.N. Pal, S. Pal. *Inorg. Chem.*, **40**, 4807 (2001).

[10] B.D. Clercq, F. Verpoort. *Adv. Synth. Catal.*, **344**, 639 (2002).

[11] B.D. Clercq, F. Lefebvre, F. Verpoort. *Appl. Catal. A*, **247**, 345 (2003).

[12] A. Patra, S. Sarkar, M.G.B. Drew, E. Zangrando, P. Chattopadhyay. *Polyhedron*, **28**, 1261 (2009).

[13] S.A. Patil, V.H. Naik, A.D. Kulkarni, P.S. Badami. *Spectrochim. Acta, Part A*, **75**, 347 (2010).

[14] A.K. Nandi, S. Chaudhuri, S.K. Mazumdar, S. Ghosh. *J. Chem. Soc., Perkin Trans. 2*, **11**, 1729 (1984).

[15] M.A. Ali, D.A. Chowdhury-I, M. N. Uddin. *Polyhedron*, **3**, 595 (1984).

[16] J.P. Scovill, D.L. Klayman, C.F. Franchino. *J. Med. Chem.*, **25**, 1261 (1982).

[17] N.K. Singh, S.B. Singh. *Ind. J. Chem., Sect. A*, **40A**, 1070 (2001).

[18] R.K. Agarwal, L. Singh, D.K. Sharma. *Bioinorg. Chem. Appl.*, **2006**, 1 (2006).

[19] M.E. Hossain, M.N. Alam, J. Begum, M.A. Ali, M. Nazimuddin, F.E. Smith, R.C. Hynes. *Inorg. Chim. Acta*, **249**, 207 (1996).

[20] P. Bindu, M.R.P. Kurup, T.R. Satyakeerty. *Polyhedron*, **18**, 321 (1998).

[21] A.K. Pramanik, M.S. Jana, T.K. Mondal. *J. Coord. Chem.*, **66**, 4067 (2013).

[22] M. Kalita, P. Gogoi, P. Barman, B. Sarma. *J. Coord. Chem.*, **67**, 2445 (2014).

[23] P. Gogoi, S. Hazarika, M.J. Sarma, K. Sarma, P. Barman. *Tetrahedron*, **70**, 7484 (2014).

[24] D. Banerjee, U. Ray, S. Jasimuddin, J.C. Liou, T.H. Lu, C. Sinha. *Polyhedron*, **25**, 1299 (2006).

[25] R. Balamurugan, M. Palaniandavar, M.A. Halcrow. *Polyhedron*, **27**, 1077 (2006).

[26] B. Turner, S. Swavey. *Inorg. Chem. Commun.*, **10**, 209 (2007).

[27] M.M. Tamizh, R. Karvembu. *Inorg. Chem. Commun.*, **25**, 30 (2012).

[28] J. Hurtado, M. Portaluppi, R. Quijada, R. Rojas, M. Valderrama. *J. Coord. Chem.*, **62**, 2772 (2009).

[29] D.Y. Ma, L.X. Zhang, X.Y Rao, T.L. Wu, D.H. Li, X.Q. Xie. *J. Coord. Chem.*, **66**, 1486 (2013).

[30] K. Karami. *J. Coord. Chem.*, **63**, 3688 (2010).

[31] K.C. Gupta, A.K. Sutar. *Coord. Chem. Rev.*, **252**, 1420 (2008).

[32] S. Ray, S. Jana, A. Jana, S. Konar, K. Das, S. Chatterjee, R.J. Butcher, S.K. Kar. *Polyhedron*, **46**, 74 (2012).

[33] I.E. Marko, A. Gautier, R. Dumeunier. *Angew. Chem. Int. Ed.*, **43**, 1588 (2004).

[34] P. Gamez, I.W.C.E. Arends, J. Reedijk, R.A. Sheldon. *Chem. Commun.*, **19**, 2414 (2003).

[35] P. Belanzoni, C. Michel, E.J. Baerends. *Inorg. Chem.*, **50**, 11896 (2011).

[36] Y. Zhu, B. Zhao, Y. Shi. *Org. Lett.*, **15**, 992 (2013).

[37] J.M. Hoover, S.S. Stahl. *J. Am. Chem. Soc.*, **133**, 16901 (2011).

[38] N. Tyagi, R. Kumar, K. Mahiya, P. Mathur. *J. Coord. Chem.*, **66**, 3335 (2013).

[39] Z. Nadealian, V. Mirkhani, B. Yadollahi, M. Moghadam, S. Tangestaninejad, I.M. Baltork. *J. Coord. Chem.*, **66**, 1264 (2013).

[40] X.F. Yin, H. Lin, A.Q. Jia, Q. Chen, Q.F. Zhang. *J. Coord. Chem.*, **66**, 3229 (2013).

[41] C.K. Modi, P.M. Trivedi. *J. Coord. Chem.*, **67**, 3678 (2014).

[42] R. Benramdane, F. Benghanem, A. Ourari, S. Keraghel, G. Bouet. *J. Coord. Chem.*, **68**, 560 (2015).

[43] S. Velusamy, A. Srinivasan, T. Punniyamurthy. *Tetrahedron Lett.*, **47**, 923 (2006).

[44] P. Gamez, I.W.C.E. Arends, J. Reedijk, R.A. Sheldon. *Chem. Commun.*, 1414 (2003).

[45] P. Belanzoni, C. Michel, E.J. Baerends. *Inorg. Chem.*, **50,** 11896 (2011).

[46] A. Pui. *Synth. React. Inorg. Met.-Org. Nano-Met. Chem.*, **36**, 523 (2006).

[47] D.A. Rockcliffe, A.E. Martell. *J. Mol. Catal. A: Chem.*, **106**, 211 (1996).

[48] Q.X. Shi, R.W. Lu, Z.X. Zhang, D.F. Zhao. *Chin. Chem. Lett.*, **17**, 1045 (2006).

[49] D.D. Perrin, W.L.F. Armarego, Purification of laboratory Chemicals, 3rd Edn., Pergamon, New York (1988).

[50] G.M. Sheldrick. *Acta Crystallogr. A*, **64**, 112 (2008).

[51] G.M. Sheldrick, SHELXS-97 and SHELXL-97, Fortran Programs for Crystal Structure Solution and Refinement, University of Gottingen, Gottingen, Germany (1997).

[52] SMART, SAINT and SADABS, Bruker AXS Inc., Madison, Wisconsin, USA (2007).

[53] M.J. Frisch, G.W. Trucks, H.B. Schlegel, G.E. Scuseria, M.A. Robb, J.R. Cheeseman, G. Scalmani, V. Barone, B. Mennucci, G.A. Petersson, Gaussian 09, Revision C.01, Gaussian, Inc., Wallingford, CT (2010).

[54] P. Kamatchi, S. Selvaraj, M. Kandaswamy. *Polyhedron*, **24**, 900 (2005).

[55] P. Pattanayak, J.L. Pratihar, D. Patra, P. Brandao, V. Felix. *Inorg. Chim. Acta*, **418**, 171 (2014).

[56] P.G. Jones. *Chem. Soc. Rev.*, **13**, 157 (1984).

[57] S. Acharya, A. Kejriwal, A.N. Biswas, P. Das, D.N. Neogi, P. Bandyopadhyay. *Polyhedron*, **38**, 50 (2012).

[58] L.R. Martins, E.T. Souza, T.L. Fernandez, B. de Souza, S. Rachinski, C.B. Pinheiro, R.B. Faria, A. Casellato, S.P. Machado, A.S. Mangrich, M. Scarpellini. *Braz. Chem. Soc.*, **21**, 1218 (2010).

[59] E.A. Lewis, W.B. Tolman. *Chem. Rev.*, **104**, 1047 (2004).

[60] J.P. Klinman. *Chem. Rev.*, **96**, 2541 (1996).

[61] R.H. Holm, P. Kennepohl, E.I. Solomon. *Chem. Rev.*, **96**, 2239 (1996).

[62] K. Asami, K. Tsukidate, S. Iwatsuki, F. Tani, S. Karasawa, L. Chiang, T. Storr, F. Thomas, Y. Shimazaki. *Inorg. Chem.*, **51**, 12450 (2012).

[63] D. Das, Y.M. Lee, K. Ohkubo, W. Nam, K.D. Karlin, S. Fukuzumi. *J. Am. Chem. Soc.*, **135**, 2825 (2013).

Figure captions

Figure 1. Electronic spectra of **1** (10^{-4} M) (—), **2** (2×10^{-4} M) (—), **3** (2×10^{-4} M) (—), **4** (2×10^{-4} M) (—) and **5** (2×10^{-4} M) (—) in DMF.

Figure 2. Molecular structure of **HL** (**1**) with 50% probability ellipsoids.

Figure 3. Molecular structure of **2** with 50% probability ellipsoids.

Figure 4. Molecular structure of **5** with 50% probability ellipsoids.

Figure 5. Contour plots of HOMOs and LUMOs of **5**.

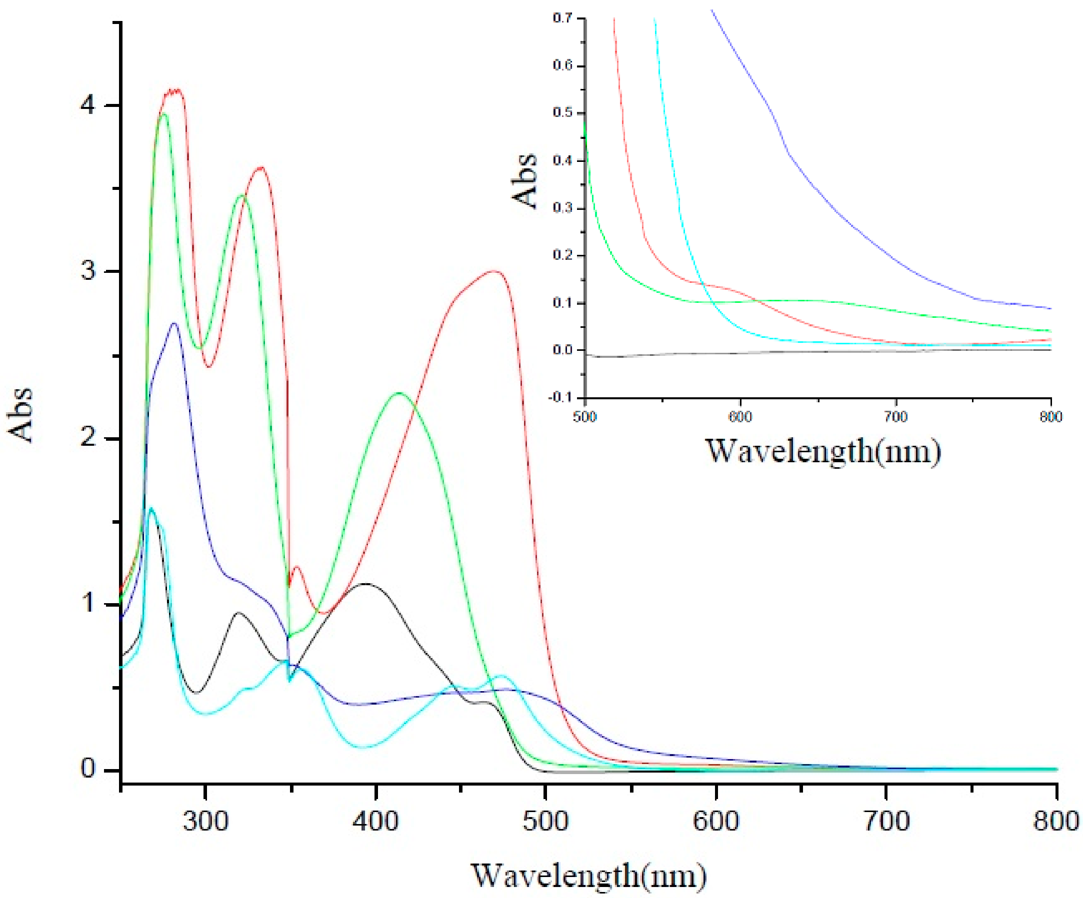

Abs
Wavelength(nm)
0
1
2
3
4
300
400
500
600
700
800
Abs
Wavelength(nm)
0.7
0.6
0.5
0.4
0.3
0.2
0.1
0.0
-0.1
500
600
700
800

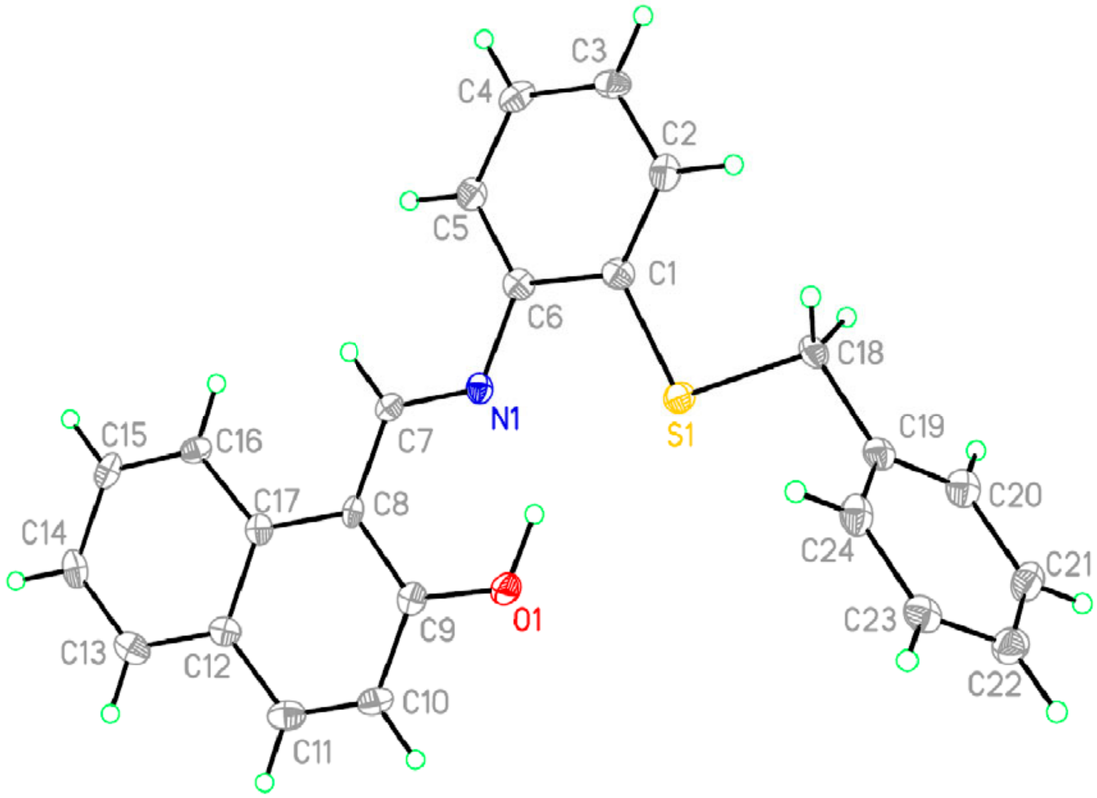
C3
C4
C2
C5
C1
C6
C18
N1
C7
S1
C15
C16
C19
C20
C17
C8
C14
C24
C21
O1
C9
C23
C13
C12
C22
C10
C11

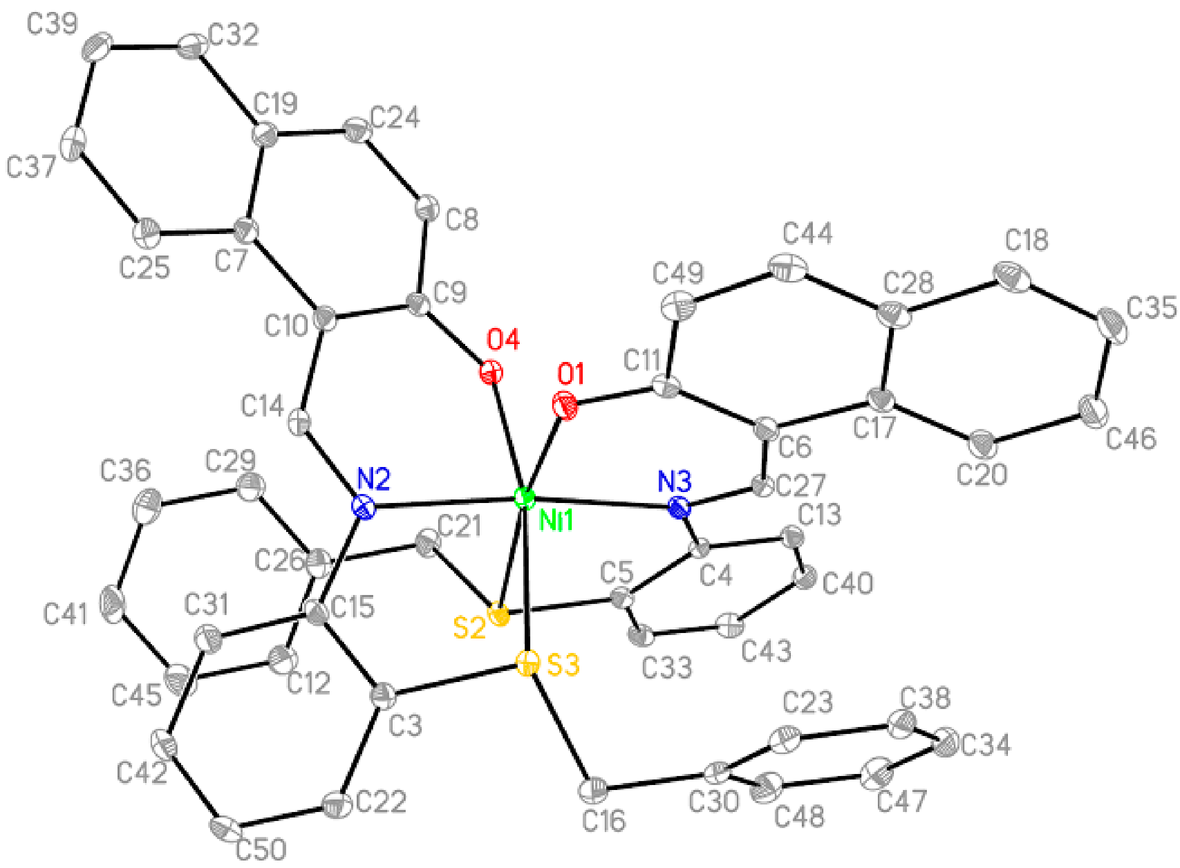
C39
C32
C19
C24
C37
C8
C25
C7
C9
C44
C18
C49
C28
C35
C10
O4
O1
C11
C14
C6
C17
C46
C36
C29
N2
N3
C27
C20
Ni1
C21
C13
C26
C5
C4
C40
C41
C31
C15
S2
C45
C12
S3
C33
C43
C3
C23
C38
C42
C34
C22
C30
C47
C16
C48
C50

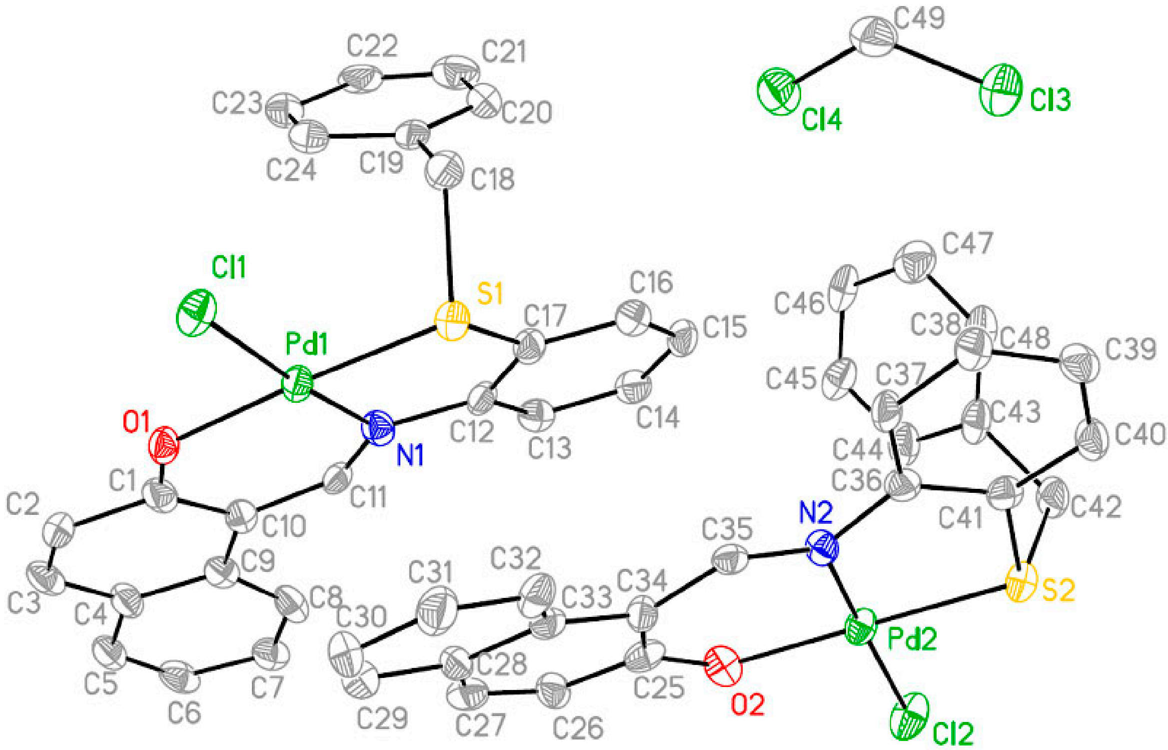
C49
Cl4
Cl3
C22
C21
C23
C20
C24
C19
C18
Cl1
S1
C17
C16
C15
Pd1
C14
O1
N1
C12
C13
C11
C1
C2
C10
C9
C8
C3
C4
C5
C6
C7
C47
C46
C38
C48
C39
C45
C37
C43
C40
C44
C36
C41
C42
C35
N2
C31
C32
C33
C34
S2
C30
Pd2
C28
C25
O2
C29
C27
C26
Cl2

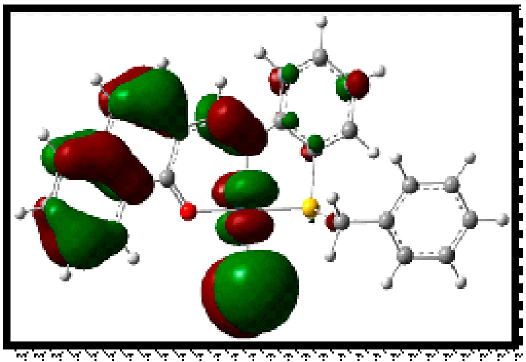

HOMO-1

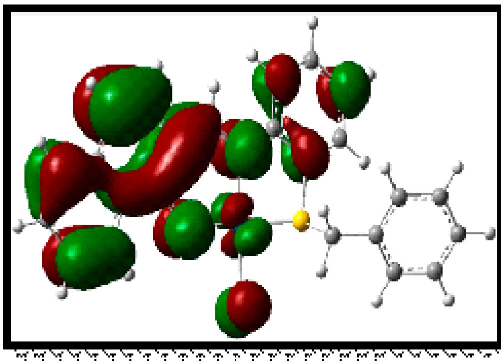

HOMO

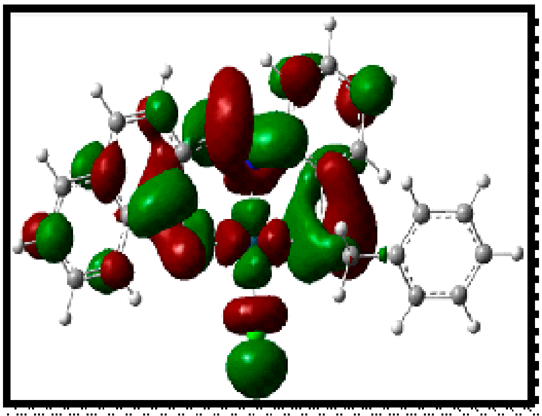

LUMO

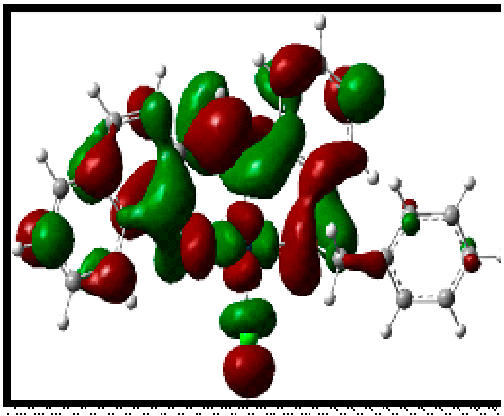

LUMO+1

Table 1. Crystal structure and structure refinement details for **1**, **2** and **5**.

Compound	**1**	**2**	**5**
CCDC entry no.	997116	997117	997118
Empirical formula	$C_{24}H_{19}NOS$	$C_{48}H_{36}N_2NiO_2S_2$	$C_{49}H_{38}Cl_4N_2O_2Pd_2S_2$
Formula weight	369.46	795.62	1105.53
T (K)	298(2)	100(2)	296(2)
λ (Å)	0.71073	0.71073	0.71073
Crystal system	Tetragonal	Triclinic	Monoclinic
Space group	P4(1)	P-1	P2(1)/c
Unit cell dimensions			
a (Å)	18.2731(8)	11.1974(5)	11.2548(7)
b (Å)	18.2731(8)	13.4777(5)	20.4902(14)
c (Å)	5.3436(3)	14.4106(6)	19.2916(11)
α (°)	90.00	96.868(3)	90.00
β (°)	90.00	110.113(4)	93.710(5)
γ (°)	90.00	110.134(4)	90.00
V ($Å^3$)	1784.25(15)	1846.20(12)	4439.6(5)
Z	4	2	4
D_{calc} (Mg/m^3)	1.375	1.431	1.654
μ (mm^{-1})	1.708	2.166	9.972
F (0 0 0)	776	828	2216
Crystal size (mm^3)	0.35 × 0.17 × 0.12	0.27 × 0.21 × 0.11	0.21 × 0.14 × 0.08
θ (°)	3.42-66.53	3.63-66.60	3.94- 66.60
Index ranges	$-21 \leq h \leq 19$ $-21 \leq k \leq 17$ $-6 \leq l \leq 4$	$-13 \leq h \leq 11$ $-12 \leq k \leq 16$ $-16 \leq l \leq 17$	$-12 \leq h \leq 13$ $-24 \leq k \leq 16$ $-22 \leq l \leq 16$
Reflections collected	4072	10570	13789
Independent reflections (R_{int})	2153(0.0547)	6445(0.0297)	7305(0.0957)
Completeness (%)	1.22/0.68	99.00	93.20
Absorption correction	Multi-scan (SADABS)	Multi-scan (SADABS)	Multi-scan (SADABS)
Max and min transmission	0.8213 and 0.5863	0.7966 and 0.5924	0.5026 and 0.2286
Refinement method	Full matrix least-squares on F^2	Full matrix least-squares on F^2	Full matrix least-squares on F^2
Data/restraints/parameters	2153 / 1 / 249	6445 / 0 / 640	7305 / 0 / 550
Goodness-of-fit on F^2	1.007	1.066	1.035
Final R indices [I>2σ(I)]	R1=0.0488, wR2=0.1055	R1=0.0352, wR2=0.1031	R1=0.0975, wR2=0.2280
Largest diff. in peak / hole ($eÅ^{-3}$)	0.241 / -0.254	0.375 / -0.394	2.102 / -0.972

Table 2. Electronic spectral data of **1**-**5**.

Compound	λ (nm)	ε_{max} ($M^{-1}cm^{-1}$)
Ligand, **1**	267	15600
	319	9490
	392	11250
	466	4020
Ni(II) complex, **2**	281	20450
	331	18050
	496	15000
	601	160
Cu(II) complex, **3**	275	19650
	320	17250
	413	11300
	652	120
Co(II) complex, **4**	281	13400
	322	5625
	485	2410
	624	500
Pd(II) complex, **5**	268	7965
	347	3000
	356	3100
	444	2575
	472	2500

Table 3. Selected bond lengths (Å) and angles (°) for **1**.

Bond lengths	(Å)	Bond angles	(°)
S(1)—C(1)	1.777(5)	C(1)—S(1)—C(18)	102.4(2)
S(1)—C(18)	1.821(5)	C(9)—O(1)—H(1A)	119(3)
O(1)—C(9)	1.343(6)	C(7)—N(1)—C(6)	122.7(4)
O(1)—H(1A)	1.020(6)	N(1)—C(6)—C(1)	115.8(4)
N(1)—C(7)	1.295(6)	N(1)—C(7)—C(8)	122.2(4)
N(1)—C(6)	1.415(6)	O(1)—C(9)—C(8)	122.1(5)
C(7)—C(8)	1.446(7)	C(19)—C(18)—S(1)	108.0(4)
C(7)—H(7)	0.930(4)		

Table 4. Selected bond lengths (Å) and angles (°) for **2**.

Bond lengths	(Å)	Bond angles	(°)
Ni—O(1)	1.9979(15)	O(1)—Ni(1)—O(4)	93.03(6)
Ni—O(4)	2.0074(14)	O(1)—Ni(1)—N(3)	90.69(6)
Ni—N(3)	2.0235(17)	O(4)—Ni(1)—N(3)	96.32(6)
Ni—N(2)	2.0281(17)	O(1)—Ni(1)—N(2)	93.83(7)
Ni—S(2)	2.4390(6)	O(4)—Ni(1)—N(2)	88.20(6)
Ni—S(3)	2.5267(6)	N(3)—Ni(1)—N(2)	173.43(7)
O(1)—C(11)	1.287(3)	O(1)—Ni(1)—S(2)	172.70(5)
O(4)—C(9)	1.288(3)	O(4)—Ni(1)—S(2)	92.54(4)
N(2)—C(14)	1.304(3)	N(3)—Ni(1)—S(2)	84.00(5)
N(2)—C(15)	1.423(2)	N(2)—Ni(1)—S(2)	91.06(5)
N(3)—C(27)	1.308(3)	O(1)—Ni(1)—S(3)	84.66(4)
N(3)—C(4)	1.421(3)	O(4)—Ni(1)—S(3)	167.32(4)
S(2)—C(5)	1.778(2)	N(3)—Ni(1)—S(3)	96.17(5)
S(2)—C(21)	1.839(2)	N(2)—Ni(1)—S(3)	79.53(5)
S(3)—C(3)	1.775(2)	S(2)—Ni(1)—S(3)	90.910(19)
S(3)—C(16)	1.833(2)		

Table 5. Selected bond lengths (Å) and angles (°) for **5**.

Bond lengths	(Å)	Bond angles	(°)
Pd(1)—O(1)	2.004(8)	O(1)—Pd(1)—N(1)	92.9(3)
Pd(1)—N(1)	2.010(9)	O(1)—Pd(1)—S(1)	176.7(2)
Pd(1)—S(1)	2.231(3)	N(1)—Pd(1)—S(1)	87.6(3)
Pd(1)—Cl(1)	2.322(3)	O(1)—Pd(1)—Cl(1)	89.1(2)
Pd(2)—O(2)	1.978(9)	N(1)—Pd(1)—Cl(1)	175.8(3)
Pd(2)—N(2)	2.004(8)	S(1)—Pd(1)—Cl(1)	90.60(10)
Pd(2)—S(2)	2.232(3)	O(2)—Pd(2)—N(2)	93.0(4)
Pd(2)—Cl(2)	2.330(3)	O(2)—Pd(2)—S(2)	179.5(3)
S(2)—C(41)	1.793(11)	N(2)—Pd(2)—S(2)	87.0(3)
S(2)—C(42)	1.854(13)	O(2)—Pd(2)—Cl(2)	89.0(3)
S(1)—C(17)	1.779(11)	N(2)—Pd(2)—Cl(2)	176.3(3)
S(1)—C(18)	1.854(12)	S(2)—Pd(2)—Cl(2)	90.92(11)
Cl(4)—C(49)	1.730(15)		
Cl(3)—C(49)	1.788(16)		
O(1)—C(1)	1.269(15)		
O(2)—C(25)	1.321(16)		
N(2)—C(35)	1.303(15)		
N(2)—C(36)	1.428(15)		
N(1)—C(11)	1.279(16)		
N(1)—C(12)	1.436(14)		

Table 6. Optimized reaction condition for benzyl alcohol to benzyldehyde at room temperature.

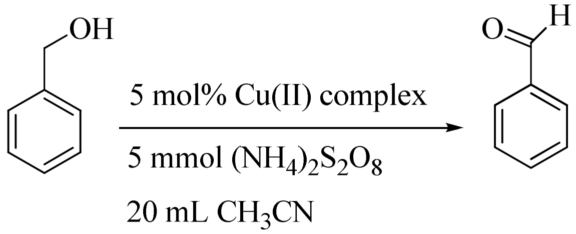

Entry	Catalyst	Oxidant	Solvent	Time	Conversion%	Yield
1	None	$(NH_4)_2S_2O_8$	CH_3CN	24 h	0	0
2	$CuCl_2$	$(NH_4)_2S_2O_8$	CH_3CN	4 h	56	50
3	**Cu(II) Complex**	**$(NH_4)_2S_2O_8$**	**CH_3CN**	**2 min**	**100**	**96**
4	Cu(II) Complex	H_2O_2	CH_3CN	2 h	80	71
5	Cu(II) Complex	$(NH_4)_2S_2O_8$	CH_2Cl_2	15 min	82	74
6	Cu(II) Complex	$(NH_4)_2S_2O_8$	DMF	30 min	40	29
7	Cu(II) Complex	$(NH_4)_2S_2O_8$	DMSO	30 min	42	32
8	Cu(II) Complex	$(NH_4)_2S_2O_8$	THF	30 min	51	41

Table 7. Oxidation of alcohol to aldehyde catalyzed by Cu(II) complex in CH_3CN-$(NH_4)_2S_2O_8$ system.

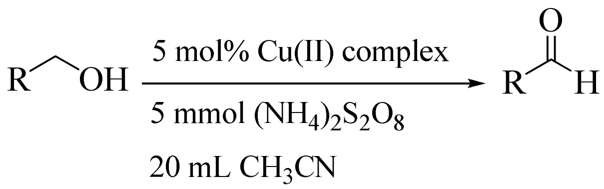

Entry	Substrate	Product	Time (min)	Yield (%)
1	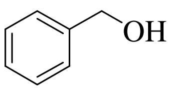	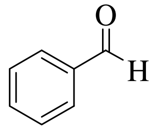	2	96
2	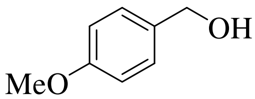	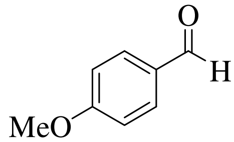	3	92
3	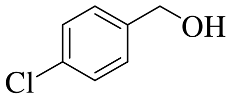	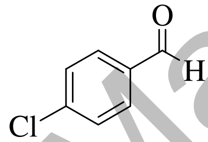	5	86
4	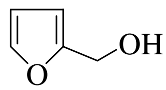	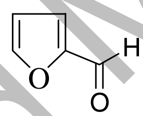	4	86
5	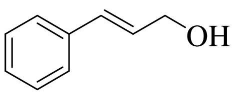	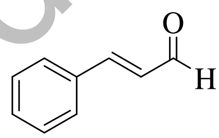	6	92
6	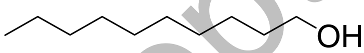	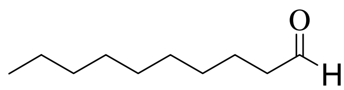	4	92
7	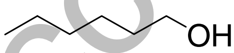	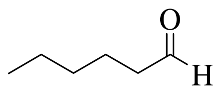	4	91
8	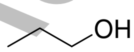	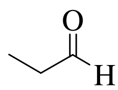	3	89
9	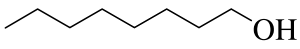	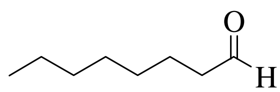	4	93

Table 8. The experimental and calculated bond lengths (Å) and angles (°) for **5**.

Bond lengths	Expt	Calcd	Bond angles	Expt	Calcd
Pd(1)—O(1)	2.004(8)	2.028	O(1)—Pd(1)—N(1)	92.9(3)	93.69
Pd(1)—N(1)	2.010(9)	2.043	O(1)—Pd(1)—S(1)	176.7(2)	178.73
Pd(1)—S(1)	2.231(3)	2.303	N(1)—Pd(1)—S(1)	87.6(3)	86.64
Pd(1)—Cl(1)	2.322(3)	2.358	O(1)—Pd(1)—Cl(1)	89.1(2)	90.20
S(1)—C(17)	1.779(11)	1.797	N(1)—Pd(1)—Cl(1)	175.8(3)	175.77
S(1)—C(18)	1.854(12)	1.883	S(1)—Pd(1)—Cl(1)	90.60(10)	89.51
O(1)—C(1)	1.269(15)	1.283			
N(1)—C(11)	1.279(16)	1.321			
N(1)—C(12)	1.436(14)	1.420			

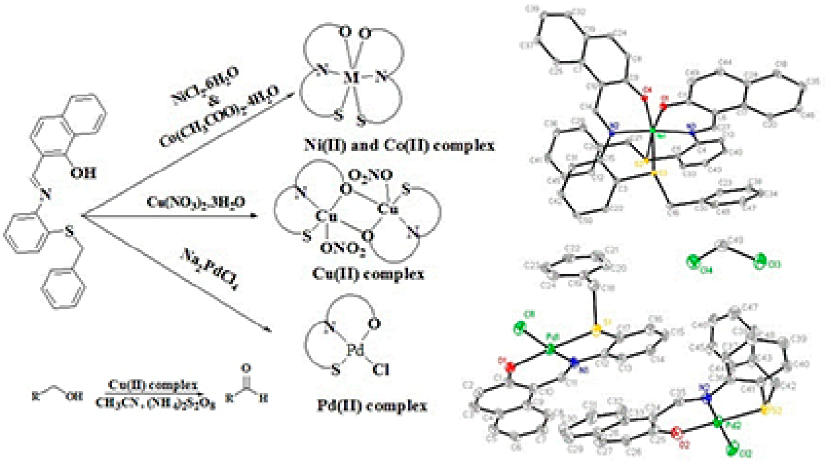
OH
N
S
NiCl2.6H2O
&
Co(CH3COO)2.4H2O
Ni(II) and Co(II) complex
Cu(NO3)2.3H2O
Cu(II) complex
Na2PdCl4
Pd(II) complex
Cu(II) complex
CH3CN, (NH4)2S2O8